 doi:10.20944/preprints202209.0414.v1

Article

Mitigating Lithium Dissolution and Polysulfide Shuttle Effect Phenomena using a Polymer Composite Layer Coating on Anode in Lithium–Sulfur Batteries

Hyukmin Kweon[1,2,*] and William Kim-Shoemaker[3]

[1] Civil and Environmental Engineering, University of California, Los Angeles, Los Angeles, California 90095, USA
[2] BenSci Inc., 2321W 10th Street, Los Angeles, CA 90006, USA
[3] Jericho High School, 99 Cedar Swamp Rd., Jericho, NY, 11753, USA; w.kim-shoemaker@jerichoapps.org
* Correspondence: kweonhyukmin@gmail.com

Abstract: To mitigate lithium dissolution and polysulfide shuttle effect phenomena in high energy lithium sulfur batteries (LISBs), a conductive, flexible, and easily modified polymer composite layer was applied on the anode. The polymer composite layer includes polyaniline and functionalized graphite. The electrochemical behavior of LISBs was studied by galvanostatic charge/discharge tests from 1.7 to 2.8 V up to 90 cycles and via COMSOL Multiphysics simulation software. No apparent overcharge occurred during the charge state, which suggests that the shuttle effect of polysulfides was effectively prevented. The COMSOL Multiphysics simulation provides a venue for optimal prediction of the ideal concentration and properties of the polymer composite layer to be used in the LISBs. The testing and simulation results determined that the polymer composite layer diminished the amount of lithium polysulfide species and decreased the amount of dissolved lithium ions in the LISBs. In addition, the charge/discharge rate of up to 2.0 C with a cycle life of 90 cycles was achieved. The knowledge acquired in this study was important not only for the design of efficient new electrode materials, but also for understanding the effect of the polymer composite layer on the electrochemical cycle stability.

Keywords: lithium sulfur battery; polysulfide; shuttle effect; dendrite; polyaniline; graphite; COMSOL

1. Introduction

Recently, lithium-ion batteries (LIBs) have achieved great success and are used widely in electric vehicles, consumer electronics, and stationary energy storage systems.[1] Many studies have been conducted to achieve highly safe, high energy density storage systems with sustainable electrochemical performance.[2–6] The focus of most studies has been LIB modifications that improve traits such as lifespan, efficiency, and size. Highly reactive electrode/electrolyte materials provide increased power and performance, but result in fire and/or explosion and accelerated degradation even when the battery is not used.[7] In addition, improved LIBs can hardly support the growing demand for high-energy density electrochemical cells. To overcome these limitations, lithium sulfur batteries (LISBs) have been proposed as a potential alternative to current state-of-the-art LIBs due to their theoretical high capacity (1675 mAh/g) and energy density (2510 Wh/kg).[8,9] Sulfur is also considered a sustainable resource due to the low environmental impact of its harvest and the possibility of reusing sulfur from used batteries.[10] Table 1 summarizes advantages and disadvantages of both LIBs and LISBs.

Preprints (www.preprints.org) | NOT PEER-REVIEWED | Posted: 27 September 2022 doi:10.20944/preprints202209.0414.v1

Table 1. Comparison of key features of lithium-ion and lithium sulfur batteries.

Lithium-ion batteries (LIBs)	Advantage	- Light-weight (provides the same or greater energy at less than half the weight and size) [11] - Higher voltage than other rechargeable batteries[11] - Greater number of charge and discharge cycles[11] - 99% Coulombic efficiency[12]
	Disadvantage	- Fire risk [11] - Limited capacity and energy density[13] - Availability of transitional metal resources[14] - Severely damaged by deep discharge cycles[15]
Lithium sulfur batteries (LISBs)	Advantage	- Low cost, non-toxic, and natural abundance of sulfur[16] - Theoretical high capacity (1675 mAh/g)[8] - High energy density (2510 Wh/kg)[9] - 92-97% Coulombic efficiency[9]
	Disadvantage	- Lower voltage than conventional lithium-ion batteries[9] - Low cycle life[9] - Low actual energy capacity due to polysulfide phenomena[9] - Inferior reversibility due to dissolution of polysulfide into electrolytes[17]

Despite the LISB advantages, their practical implementation is hinder by the challenge of a dramatically shortened cycle life. This is mainly due to the polysulfide shuttle and lithium dissolution effects, which lead to the formation of dendrites on the lithium anodes as lithium ions return to the anode; these ions them accumulate on cathode as polysulfide species.[18,19] Together, the non-dissolvable intermediate lithium polysulfides on the sulfur cathode and uncontrollable growth of lithium dendrites on the anode surface reduce the activity of the LISBs.[20] Several approaches have been developed to address these issues over the past few decades including cathode design, separator modification, use of novel electrolytes, and anode improvement.[21] To fabricate advanced sulfur-based composite cathodes, various porous materials and conductive materials such as porous carbon material[22] and graphene-based material[23] are considered for their high electrical conductivity. A separator, usually a polymer membrane acts as an electron insulator to prevent short circuits. Modified separators have proven to be an efficient way to inhibit polysulfide shuttles.[21] In addition, the anode improvement in LISBs deserve attention from researchers. Deactivation of lithium anodes is the most common reason for failure because lithium is highly reactive to organic electrolytes and form solid electrolyte interfaces. Lithium ions dendrites form that are deposited irregularly on the lithium anode while the material is displaced.

In this study, we propose that a polymer composite layer coating on anode in LISBs to mitigate lithium dissolution and polysulfide shuttle effect phenomena. The polymer composite layer was a conductive, flexible, and easily modified materials (polyaniline; PANi, with functionalized graphite) and was applied to the surface of the pre-lithiated graphite and carbon black anode. This coating layer could withstand the volume change of lithium during the cycle and enhance the cycling ability of LISBs. In addition, the polymer composite coating materials are chemically stable enough not to dissolve in the electrolyte, and are significantly conductive.[24,25] The applied conductive polymer composite material improved the cycle life of the LISBs. Additionally, the ionic conductivity of the polymer composite layer was enhanced by a doping treatment with hydrofluoric acid (HF).[26] Hence, the doped layer can assist in the structural maintenance of the anode while preserving conductivity traits of the original relationship between the electrolyte and the anode.

Preprints (www.preprints.org) | NOT PEER-REVIEWED | Posted: 27 September 2022 doi:10.20944/preprints202209.0414.v1

2. Materials and Methods

2.1. Materials

Polyvinylidene fluoride (PVDF), n-methyl-2-pyrrolidone (NMP), carbon black, conductive acetylene black nano powder, graphite (TIMCAL TIMREX® KS6), Lithium nickel manganese cobalt oxides (NMC 424, $LiNi_{0.4}Mn_{0.2}Co_{0.4}O_2$), sulfur-carbon composite, copper foil (9 μm thickness), and aluminum foil (15 μm thickness) were purchased from MSE Supplies LLC, AZ, USA. Lithium perchlorate ($LiClO_4$), sulfolane, lithium polysulfide (Li_2S_8), and HF were purchased from Sigma-Aldrich. All chemicals were used as received without any treatment or purification.

2.2. Material Synthesis

First, a PVDF solution of was prepared in a mass ratio of 1:15 of PVDF to NMP and heated for 12 h. Then, the NMC, sulfur, and carbon black powders was ground together for the cathode in accordance with a mass ratio of 35:60:5 under continuous stirring for 2 h while heated to 155 °C. The slurry was then distributed evenly over the aluminum foil with a doctor blade and dried at 60 °C for 12 h. Next, NMC and graphite were dispersed for the anode in accordance with a mass ratio of 88:12 in a ball-milling machine. After that, the mixture was added to the PVDF solution through sonication. In this method, the degree of pre-lithiation is easily controlled by adjusting the weight ratio of the anode material and the Li metal. The slurry was cast onto a cupper foil with a doctor blade and dried at 60 °C for 24 h. The PANi composite with functionalized graphite was prepared using method by described in a previous work.[27–29] The prepared polymer composite solution was spin-coated to form a thin polymer film on the anode. Electrolytes were made by dissolving 1 M of $LiClO_4$ in sulfolane. Additionally, lithium polysulfide solutions were added within the electrolyte solution.

2.3. Electrochemical Measurements and Characterization

Coin cells (2032) were assembled in an argon-filled glovebox with moisture and oxygen contents below 3 ppm. The quantity of electrolyte was controlled at 12~15 μL per 1 mg sulfur. Galvanostatic charge/discharge tests were carried out using a LANHE battery tester (Wuhan LAND Electronic Co. Ltd.) within a voltage window of 1.7~2.8 V for up to 90 cycles. Initially, the cells were activated by discharging at a constant current of 0.1 C (1.0 C = 1675 mAh/g) to 1.7 V, and then charged at a constant current of 0.1 C to 2.8 V for three cycles. After activation, the cells were tested at 0.1 C, 0.2 C, 0.4 C, 0.6 C, 0.8 C, 1.0 C and 2.0 C, respectively. The morphologies of the electrode and coated layers were examined with a Phenom Pharos desktop field emission scanning electron microscope (FE-SEM) using a secondary electron detector (SED) from Thermo Scientific. To observe electrodes after 90 cycles were disassembled in an argon-filled glove box. All FE-SEM images were captured with 10 kV acceleration voltage.

2.4. COMSOL Multiphysics Simulation

One-dimensional (1D) battery simulation is made up of four sections: the negative electrode, polymer composite layer, separator, and the positive electrode. This model was modified from an existing implementation of a COMSOL 1D LIB model (COMSOL, Inc., Burlington, MA, Application ID: 686). It includes an isothermal system that models electronic current conduction in the electrodes, ion transport across the battery, material transport in the electrolyte, and Butler-Volmer electrode kinetics in combination with the Nernst equation (assuming law of mass action) and using experimentally measured discharge curves for the equilibrium potential. A schematic diagram of the 1D LISB model as it appears in the COMSOL program can be seen in Figure 1. The model is split into four sections, each having different thicknesses: the negative electrode (25 μm without polymer layer), polymer composite layer (5 μm), the separator (0 micrometers, represented as a point), and the positive electrode (20 μm). The model comes with default properties associated with the materials used to construct it. The electrical conductivity of metals was

Preprints (www.preprints.org) | NOT PEER-REVIEWED | Posted: 27 September 2022 doi:10.20944/preprints202209.0414.v1

assumed to be effective and to constantly account for the porous nature of the matrix. The diffusion coefficient was set to 1×10^{-9} m^2/s.

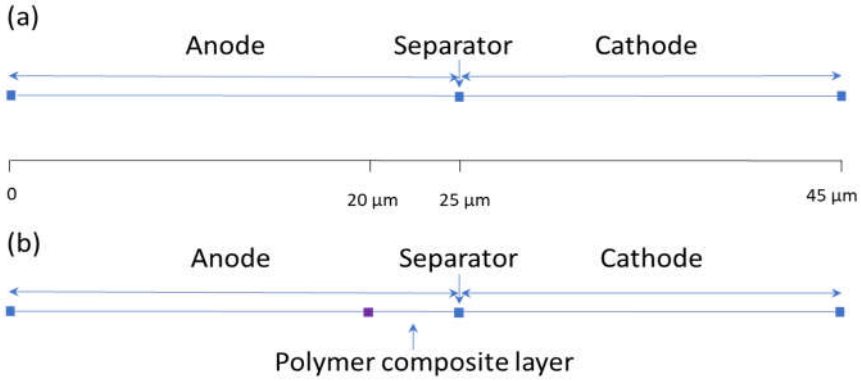

Figure 1. A schematic diagram of the 1D LISBs as they appear on COMSOL: (**a**) Without polymer composite layer; (**b**) With polymer composite layer.

To create and plot the cell voltage data, cell voltage was selected in the 1D plot group setting and the plot chosen. To find all species concentrations, the default plot was modified to show the concentrations for the last saved time, and for each C-rate individually. Computing the results from the study produced results for lithium concentration as well as the polysulfide volume fraction in the electrolyte, which were graphed and plotted with the provided COMSOL functions.

3. Results and Discussion

A pure lithium metal is an ideal anode material; however, the significant volume change due to the dendritic growth can lead to the pulverization of the anode and the expansion of the cell case, which may cause sudden failure and a serious safety hazard.[30,31] To avoid the cell expansion, use of non-lithium anode is an alternative approach out of the primary dilemma of lithium metal anode. Various lithium sources such as lithium chloride (LiCl), lithium hydroxide (LiOH), lithium cobalt (LiCo), lithium oxide (LiO), and lithium metal were used as additives for a passive pre-lithiation to improve initial coulombic efficiency. In this study, pre-lithiated graphite and carbon black anode powder additives were utilized, which results in a high-rate capacity and low cost.

A fixed amount of lithium composite materials was applied and deposited onto the metal substrates using the doctor blade (20 µm thickness), then a subsequent polymer composite material coat was added using a spin coater. Figure 2 illustrates the morphology differences between the anodes without and with the polymer composite layer. The pristine pre-lithiated graphite and carbon black anode in Figure 2 (a) has a bumpy surface with irregular thickness, whereas the polymer composite coated pristine pre-lithiated graphite and carbon black anode in Figure 2 (b) has dense and flat surface. As shown in Figure 2 (b), notably thin coatings (less than 5 µm) are necessary to ensure the benefit of higher energy storage capacity of the lithium composite anode.[32]

Preprints (www.preprints.org) | NOT PEER-REVIEWED | Posted: 27 September 2022 doi:10.20944/preprints202209.0414.v1

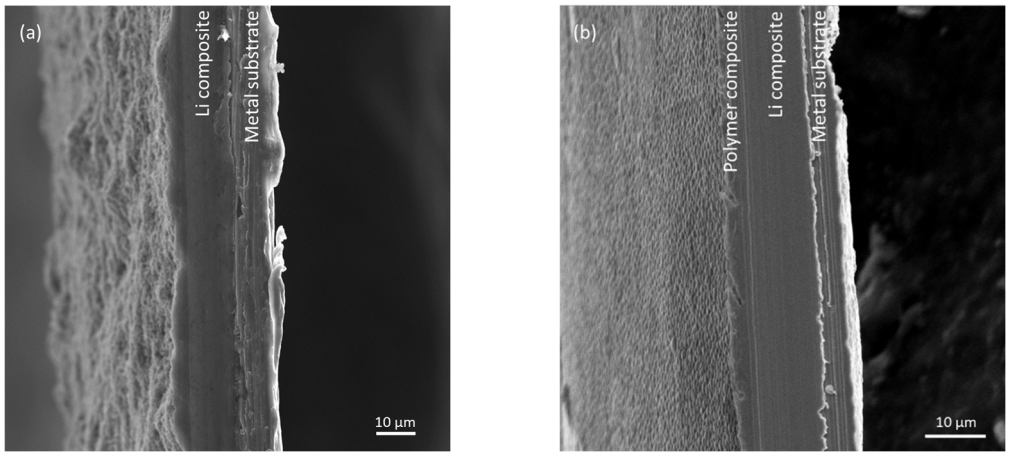

(**a**) (**b**)

Figure 2. Cross sectional SEM images of anodes: (**a**) Pristine pre-lithiated graphite and carbon black anode; (**b**) Polymer composite coated on the pre-lithiated graphite and carbon black anode.

X-ray photoelectron spectroscopy (XPS) was utilized to further confirm and characterize the polymer coating layer on the surface of the electrode. In the C1s peaks of the pristine pre-lithiated graphite and carbon black anode (Figure 3 (a)), three peaks were located at 284.5, 286.7, and 288.5 eV, which correspond to the carbon-carbon (C=C) bond from graphite and a carbon-oxygen (C-O) and C=O bonds of lithium carbonates, respectively. In the case of the polymer composite coated anode (Figure 3 (b)), an analysis of the C1s orbital energies provided evidence of an amide functional group in polyaniline composite coating layer; carbon-nitrogen (C–N) appears at 285.7 eV and isocyanic acid (HN-C=O) appears at 287.9 eV, respectively. In addition, a new peak appeared at 289.8 eV, which is attributed to the carbon-fluorine (C-F) bonds from the HF doping of the polymer composite coating layer. After coating with polymer composite material, the peak of C=C at 284.5 eV was relatively small due to the formation of new polymer composite layer. The SEM and XPS results support the successful formation of new polymer composite layer on the pristine pre-lithiated graphite and carbon black anode.

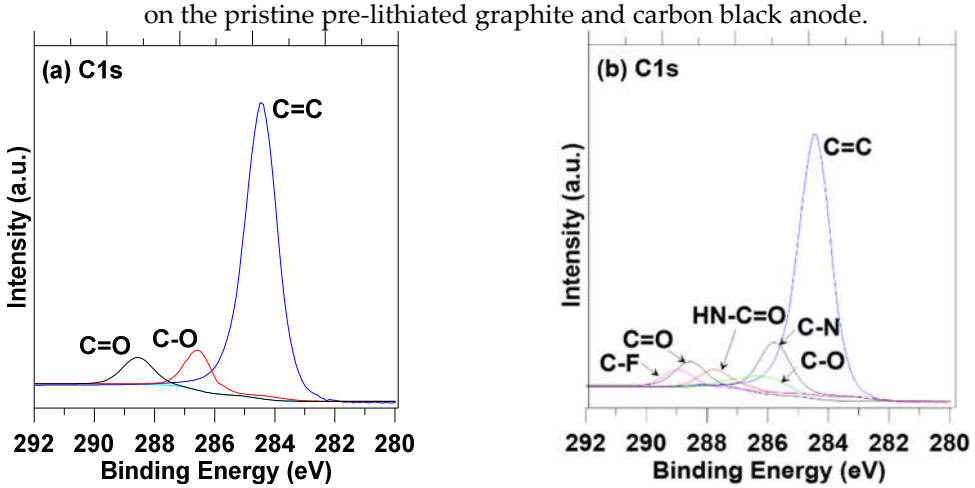

(**a**) (**b**)

Figure 3. XPS spectra of the following: (**a**) Pristine pre-lithiated graphite and carbon black anode; (**b**) Polymer composite coated pre-lithiated graphite and carbon black anode.

The galvanostatic charge/discharge tests were carried out to measure the electrochemical performance and profiles from 1.7 to 2.8 V for up to 90 cycles. The galvanostatic discharge curves of the pre-lithiated graphite and carbon black anode without and with the polymer composite layer at various currents (0.1 C, 0.2 C, 0.4 C, 0.6 C, 0.8 C, 1.0 C and 2.0 C) are shown in Figure 4 (a) and (b). The reversible discharge capacity without the

Preprints (www.preprints.org) | NOT PEER-REVIEWED | Posted: 27 September 2022 doi:10.20944/preprints202209.0414.v1

polymer composite layer can reach up to 1368 mAh/g at 0.2 C. With an increase in current density, the specific capacity gradually decreases to 1266 mAh/g (0.4 C), 1182 mAh/g (0.6 C), 1108 mAh/g (0.8 C), 1012 mAh/g (1.0 C) and 608 mAh/g (2.0 C), respectively (Figure 4 (a)). On the other hand, Figure 4 (b) shows that the reversible discharge capacity with the polymer composite layer can reach up to 1308 mAh/g at 0.2 C. As the current density is increased, the specific capacity gradually decreases to 1230 mAh/g (0.4 C), 1160 mAh/g (0.6 C), 1082 mAh/g (0.8 C), 998 mAh/g (1.0 C) and 580 mAh/g (2.0 C), respectively. No apparent overcharge occurred during the charge state, which suggests that the shuttle effect of polysulfides was effectively prevented. Once the current density goes back to 0.2 C, the specific capacity without the polymer composite layer recovers from 1368 mAh/g to 1352 mAh/g; whereas, the specific capacity with the polymer composite layer recovers from 1308 mAh/g to 1302 mAh/g, respectively. These results demonstrate the outstanding rate performance of the pre-lithiated graphite and carbon black anode with the polymer composite layer electrode. Figure 4 (c) presents the rate performance of two electrodes. Note that the discharge capacity decreases obviously during the first a couple of cycles before reaching a steady state. Both electrodes exhibit stable behaviors from 0.2 C to 2.0 C up to 90 cycles, maintaining their initial capacities. The capacity of the high-potential plateau decreases slightly with the increased rate for 2.0 C and 1.0 C, but remains nearly constant for 0.8 C, 0.6 C, 0.4 C, and 0.2 C.

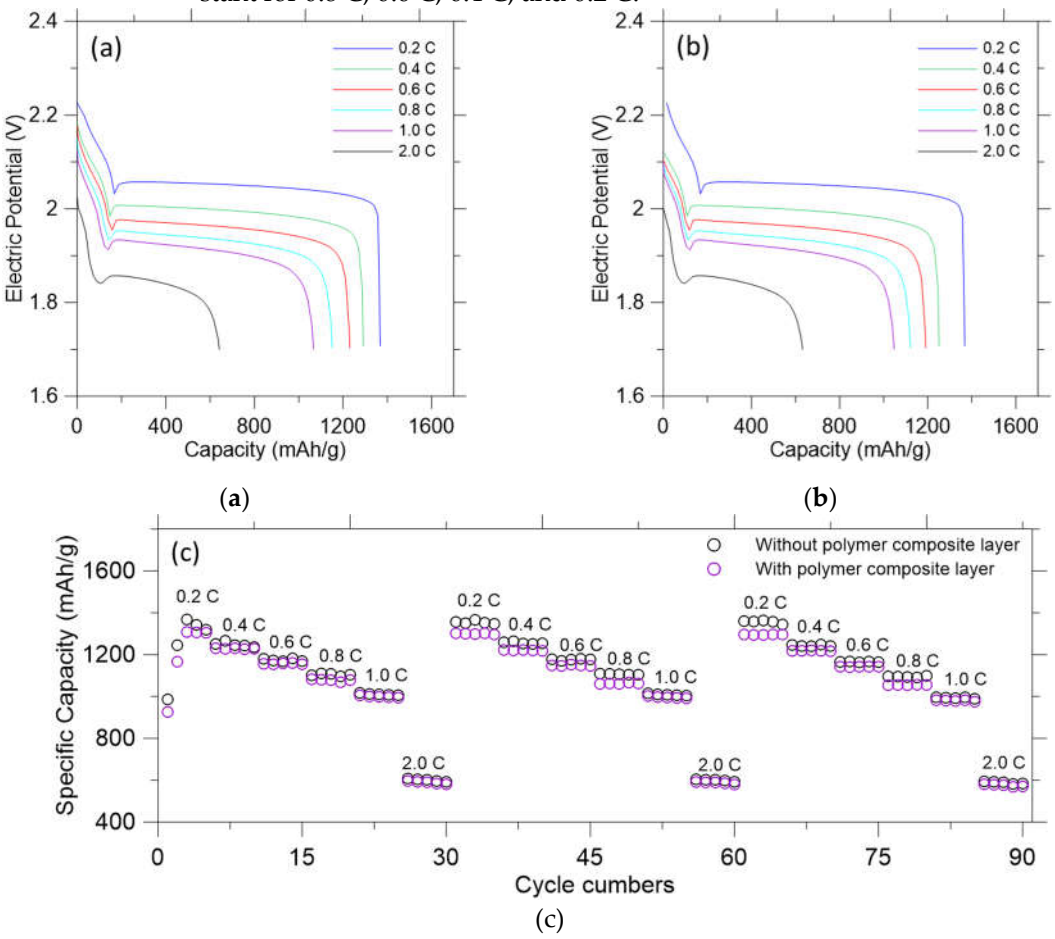

Figure 4. Electrochemical performance of the LISBs experimentally. Initial galvanostatic discharge profiles: (**a**) Without the polymer composite layer; (**b**) With the polymer composite layer. (**c**) Rate performance at current density from 0.2 C to 2 C without and with the polymer composite layer.

The 1D COMSOL model was built to further evaluate the role of a polymer composite layer in the proposed LISBs. The first parameter was the diffusion coefficient of the electrode without and with the polymer composite layer. The diffusion coefficient did have a significant effect on discharge curves. The discharge curve presents the voltage

Preprints (www.preprints.org) | NOT PEER-REVIEWED | Posted: 27 September 2022 doi:10.20944/preprints202209.0414.v1

discharged for the capacity remaining in the LISBs. As shown in the Figure 5, each curve corresponds to battery discharge according to different current densities from 0.2 C to 2.0 C. Whether there is the polymer composite layer or not, the discharge curves were not affected at the higher diffusion coefficients. However, lower diffusion coefficient could not output as much voltage at higher currents due to fewer ions crossing the separator at the low diffusion coefficient. The similar predicted discharge curves indicate that the presence of the polymer composite layer does not affect the discharge or energy production of the LISBs.

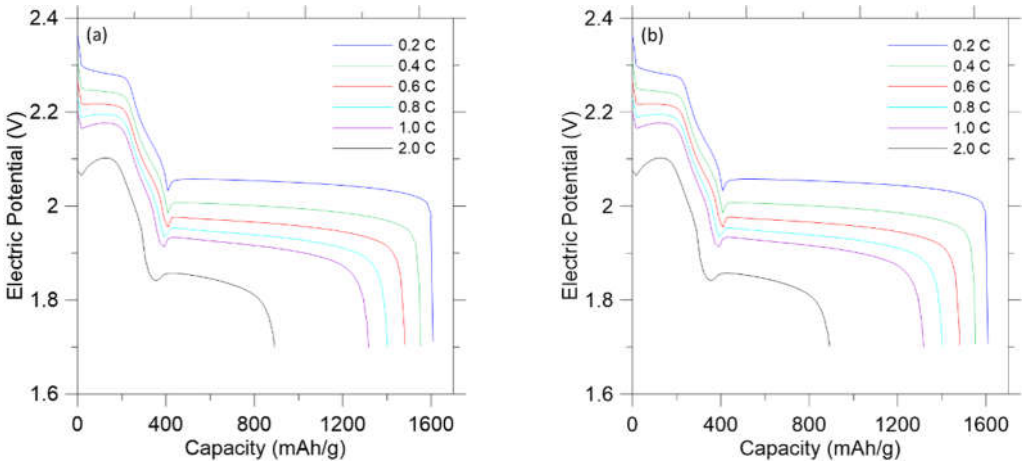

(**a**) (**b**)

Figure 5. Discharge curves of LISBs at densities varying from 0.2 C to 2.0 C from the COMSOL model: (**a**) Without the polymer composite layer; (**b**) With the polymer composite layer.

As reported in the literature, the solubility of polysulfide is one of the capacity fading factors which are the main cause of the current low energy capacity of LISBs.[33,34] This solubility causes a polysulfide shuttle phenomenon that (1) delays completion of a charging process, (2) reduces utilization of an active material in a discharging process, and (3) contributes to capacity fading.[35] One more significant factor of capacity fading is the irreversible precipitate (for example, lithium sulfide, Li_2S) on the cathode, which is insoluble and electrochemically inaccessible. Therefore, the lithium sulfide was evaluated to determine whether the polymer composite layer on the anode affects the dissolution occurring. Figure 6 represents the volume of lithium sulfide species in the 1D LISBs. Without the polymer composite layer (Figure 6 (a)), a high volume fraction (0.37) of harmful lithium sulfide can be observed in the electrolyte. However, with the polymer composite layer present, a lower volume fraction (0.34) of the harmful lithium sulfide in the electrolyte (Figure 6 (b)) can be seen. This indicates that the polymer composite layer has a positive effect of generating smaller volume of the lithium sulfide in the LISBs. The reduced lithium sulfide content in the battery system will reduce the polysulfide shuttle phenomenon effect in the LISBs.

Preprints (www.preprints.org) | NOT PEER-REVIEWED | Posted: 27 September 2022 doi:10.20944/preprints202209.0414.v1

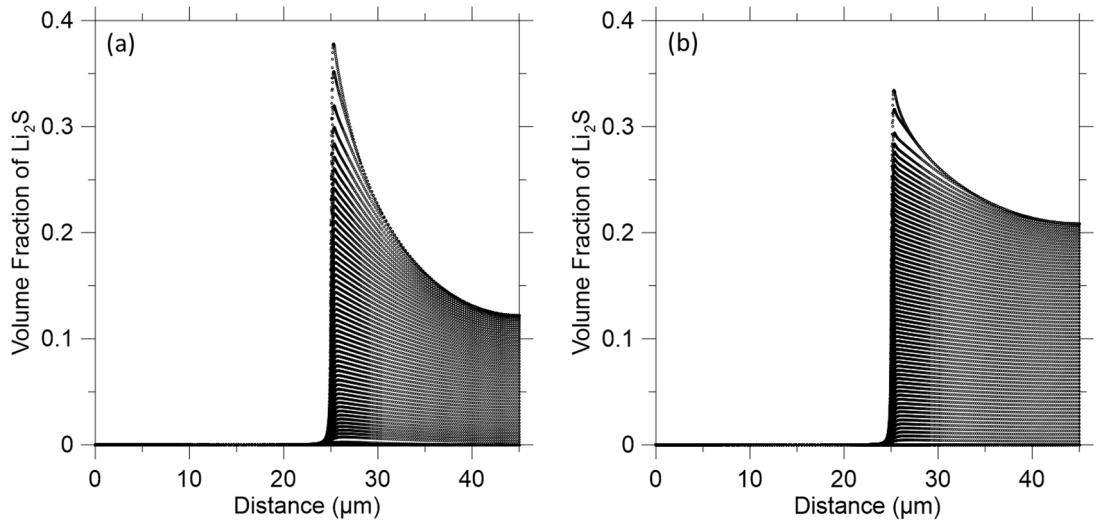

(**a**) (**b**)

Figure 6. Lithium polysulfide volume fraction on the cathode: (**a**) Without the polymer composite layer; (**b**) With the polymer composite layer.

Although the effect of the polymer composite layer on the discharge curve and volume fraction of lithium sulfide was confirmed, it is necessary to validate the effect of the polymer composite layer on the anode. Therefore, lithium concentration on both electrodes was evaluated. It was found that there was a lithium peak of 9500 mol/m^3 on the anode without the polymer composite layer (Figure 7 (a)). With the polymer composite layer, the lithium peak was 14000 mol/m^3 on the anode (Figure 7 (b)). This suggests that the polymer composite layer suppresses the dissolution of lithium ions in the electrolyte. In summary, the polymer composite layer diminishes not only the amount of polysulfide species on cathode, but also decreases the amount of dissolved lithium ions on the anode. These could be achieved without jeopardizing the total energy to be produced from the LISBs.

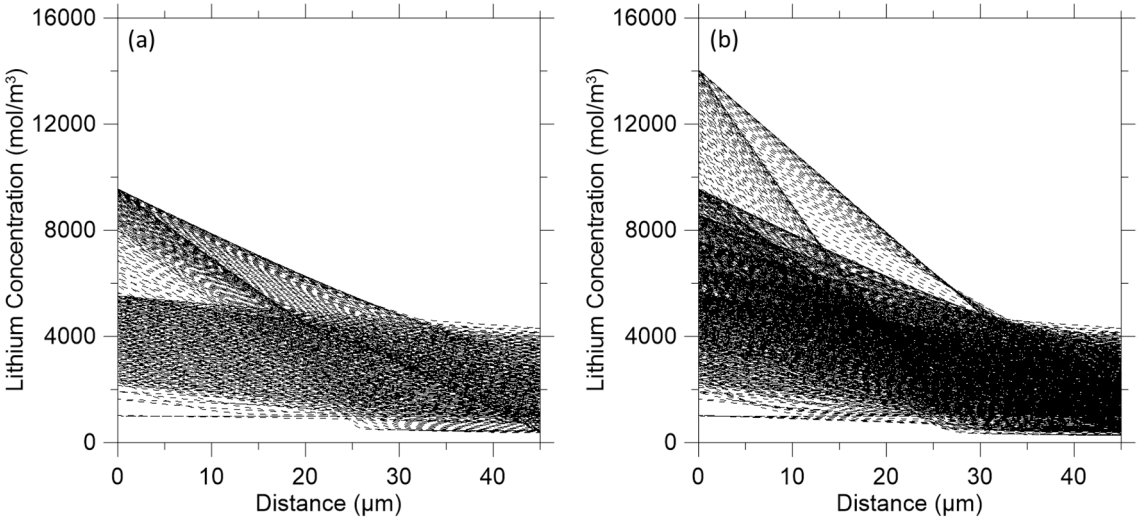

(**a**) (**b**)

Figure 7. Distribution of lithium concentration on both electrodes: (**a**) Without the polymer composite layer on the anode; (**b**) With the polymer composite layer on the anode.

4. Conclusions

A conductive, flexible, and easily modified polymer composite layer was proposed to mitigate lithium dissolution and the polysulfide shuttle effect phenomena for the LISBs. The electrochemical behavior of LISBs was studied by galvanostatic charge/discharge

tests and COMSOL Multiphysics simulation. The charge/discharge rate of up to 2.0 C with a cycle life of 90 cycles can be achieved. Additionally, overcharge was not observed during the charge state which means that the shuttle effect of polysulfides was effectively avoided. Additionally, the developed COMSOL Multiphysics simulation provides a venue for optimally predicting the ideal concentration and properties of the polymer composite material layer used in LISBs. The polymer composite layer diminishes not only the amount of lithium from anode to electrolyte, but also decreases the amount of lithium polysulfide generation on the cathode. The reduced lithium polysulfide content in the battery system will lower the polysulfide shuttle phenomenon effect in the LISBs resulting increasing the likelihood of achieving high energy density LISBs. The LISB knowledge acquired in this study contribute to the tremendous potential for battery innovative designs as storage systems for electric vehicle projects or those that utilize renewable energies such as solar, wind and wave power.

Author Contributions: Conceptualization, H.K. and W.K-S.; methodology, H.K. and W.K-S.; software, W.K-S.; validation, H.K. and W.K-S.; formal analysis, H.K. and W.K-S.; investigation, H.K. and W.K-S.; resources, H.K. and W.K-S.; data curation, H.K. and W.K-S.; writing—original draft preparation, H.K.; writing—review and editing, H.K. and W.K-S.; visualization, H.K.; supervision, H.K.; project administration, H.K. and W.K-S.; funding acquisition, H.K. and W.K-S. All authors have read and agreed to the published version of the manuscript.

Funding: This research received no external funding.

Data Availability Statement: Not applicable.

Acknowledgments: We would like to express our very great appreciation to Dr. McCalla for her valuable and constructive suggestions during the planning and development of this research work.

Conflicts of Interest: The authors declare no conflict of interest.

References

1. Li, Y.; Fu, K. "Kelvin"; Chen, C.; Luo, W.; Gao, T.; Xu, S.; Dai, J.; Pastel, G.; Wang, Y.; Liu, B.; et al. Enabling High-Areal-Capacity Lithium–Sulfur Batteries: Designing Anisotropic and Low-Tortuosity Porous Architectures Available online: https://pubs.acs.org/doi/pdf/10.1021/acsnano.7b01172 (accessed on 21 August 2022).
2. Shen, W.; Li, K.; Lv, Y.; Xu, T.; Wei, D.; Liu, Z. Highly-Safe and Ultra-Stable All-Flexible Gel Polymer Lithium Ion Batteries Aiming for Scalable Applications. *Advanced Energy Materials* **2020**, *10*, 1904281, doi:10.1002/aenm.201904281.
3. Zhang, X.; Sun, Q.; Zhen, C.; Niu, Y.; Han, Y.; Zeng, G.; Chen, D.; Feng, C.; Chen, N.; Lv, W.; et al. Recent Progress in Flame-Retardant Separators for Safe Lithium-Ion Batteries. *Energy Storage Materials* **2021**, *37*, 628–647, doi:10.1016/j.ensm.2021.02.042.
4. Song, X.; Zhang, H.; Jiang, D.; Yang, L.; Zhang, J.; Yao, M.; Ji, X.; Wang, G.; Zhang, S. Enhanced Transport and Favorable Distribution of Li-Ion in a Poly(Ionic Liquid) Based Electrolyte Facilitated by Li1.3Al0.3Ti1.7(PO4)3 Nanoparticles for Highly-Safe Lithium Metal Batteries. *Electrochimica Acta* **2021**, *368*, 137581, doi:10.1016/j.electacta.2020.137581.
5. Zou, Y.; Cao, Z.; Zhang, J.; Wahyudi, W.; Wu, Y.; Liu, G.; Li, Q.; Cheng, H.; Zhang, D.; Park, G.-T.; et al. Interfacial Model Deciphering High-Voltage Electrolytes for High Energy Density, High Safety, and Fast-Charging Lithium-Ion Batteries. *Advanced Materials* **2021**, *33*, 2102964, doi:10.1002/adma.202102964.
6. Zhao, Y.-M.; Yue, F.-S.; Li, S.-C.; Zhang, Y.; Tian, Z.-R.; Xu, Q.; Xin, S.; Guo, Y.-G. Advances of Polymer Binders for Silicon-Based Anodes in High Energy Density Lithium-Ion Batteries. *InfoMat* **2021**, *3*, 460–501, doi:10.1002/inf2.12185.
7. Ge, S.; Leng, Y.; Liu, T.; Longchamps, R.S.; Yang, X.-G.; Gao, Y.; Wang, D.; Wang, D.; Wang, C.-Y. A New Approach to Both High Safety and High Performance of Lithium-Ion Batteries. *Science Advances* **2020**, *6*, eaay7633, doi:10.1126/sciadv.aay7633.
8. Wang, R.-Y.; Kang, H.; Park, M.J. High-Capacity, Sustainable Lithium–Sulfur Batteries Based on Multifunctional Polymer Binders. *ACS Appl. Energy Mater.* **2021**, *4*, 2696–2706, doi:10.1021/acsaem.0c03244.
9. Zhu, K.; Wang, C.; Chi, Z.; Ke, F.; Yang, Y.; Wang, A.; Wang, W.; Miao, L. How Far Away Are Lithium-Sulfur Batteries From Commercialization? *Frontiers in Energy Research* **2019**, *7*.
10. Benítez, A.; Amaro-Gahete, J.; Chien, Y.-C.; Caballero, Á.; Morales, J.; Brandell, D. Recent Advances in Lithium-Sulfur Batteries Using Biomass-Derived Carbons as Sulfur Host. *Renewable and Sustainable Energy Reviews* **2022**, *154*, 111783, doi:10.1016/j.rser.2021.111783.
11. Pramanik, P.K.D.; Sinhababu, N.; Mukherjee, B.; Padmanaban, S.; Maity, A.; Upadhyaya, B.K.; Holm-Nielsen, J.B.; Choudhury, P. Power Consumption Analysis, Measurement, Management, and Issues: A State-of-the-Art Review of Smartphone Battery and Energy Usage. *IEEE Access* **2019**, *7*, 182113–182172, doi:10.1109/ACCESS.2019.2958684.
12. Xiao, J.; Li, Q.; Bi, Y.; Cai, M.; Dunn, B.; Glossmann, T.; Liu, J.; Osaka, T.; Sugiura, R.; Wu, B.; et al. Understanding and Applying Coulombic Efficiency in Lithium Metal Batteries. *Nat Energy* **2020**, *5*, 561–568, doi:10.1038/s41560-020-0648-z.

13. Fang, H. Challenges with the Ultimate Energy Density with Li-Ion Batteries. *IOP Conf. Ser.: Earth Environ. Sci.* **2021**, *781*, 042023, doi:10.1088/1755-1315/781/4/042023.
14. Weil, M.; Ziemann, S.; Peters, J. The Issue of Metal Resources in Li-Ion Batteries for Electric Vehicles. In *Green Energy and Technology*; 2018; pp. 59–74 ISBN 978-3-319-69949-3.
15. Dalal, M.; Ma, J.; He, D. Lithium-Ion Battery Life Prognostic Health Management System Using Particle Filtering Framework. *Proceedings of the Institution of Mechanical Engineers, Part O: Journal of Risk and Reliability* **2011**, *225*, 81–90, doi:10.1177/1748006XJRR342.
16. Aaldering, L.J.; Song, C.H. Tracing the Technological Development Trajectory in Post-Lithium-Ion Battery Technologies: A Patent-Based Approach. *Journal of Cleaner Production* **2019**, *241*, 118343, doi:10.1016/j.jclepro.2019.118343.
17. Sun, K.; Cama, C.A.; DeMayo, R.A.; Bock, D.C.; Tong, X.; Su, D.; Marschilok, A.C.; Takeuchi, K.J.; Takeuchi, E.S.; Gan, H. Interaction of FeS2 and Sulfur in Li-S Battery System. *J. Electrochem. Soc.* **2016**, *164*, A6039, doi:10.1149/2.0041701jes.
18. Kim, S.; Lim, W.-G.; Cho, A.; Jeong, J.; Jo, C.; Kang, D.; Han, S.M.; Han, J.W.; Lee, J. Simultaneous Suppression of Shuttle Effect and Lithium Dendrite Growth by Lightweight Bifunctional Separator for Li–S Batteries. *ACS Appl. Energy Mater.* **2020**, *3*, 2643–2652, doi:10.1021/acsaem.9b02350.
19. Suzanowicz, A.M.; Mei, C.W.; Mandal, B.K. Approaches to Combat the Polysulfide Shuttle Phenomenon in Li–S Battery Technology. *Batteries* **2022**, *8*, 45, doi:10.3390/batteries8050045.
20. Yu, S.-H.; Huang, X.; Brock, J.D.; Abruña, H.D. Regulating Key Variables and Visualizing Lithium Dendrite Growth: An Operando X-Ray Study. *J. Am. Chem. Soc.* **2019**, *141*, 8441–8449, doi:10.1021/jacs.8b13297.
21. He, Y.; Chang, Z.; Wu, S.; Zhou, H. Effective Strategies for Long-Cycle Life Lithium–Sulfur Batteries. *J. Mater. Chem. A* **2018**, *6*, 6155–6182, doi:10.1039/C8TA01115J.
22. Ji, X.; Lee, K.T.; Nazar, L.F. A Highly Ordered Nanostructured Carbon–Sulphur Cathode for Lithium–Sulphur Batteries. *Nature Mater* **2009**, *8*, 500–506, doi:10.1038/nmat2460.
23. Chen, H.; Chen, C.; Liu, Y.; Zhao, X.; Ananth, N.; Zheng, B.; Peng, L.; Huang, T.; Gao, W.; Gao, C. High-Quality Graphene Microflower Design for High-Performance Li–S and Al-Ion Batteries. *Advanced Energy Materials* **2017**, *7*, 1700051, doi:10.1002/aenm.201700051.
24. Konwer, S.; Gogoi, J.P.; Kalita, A.; Dolui, S.K. Synthesis of Expanded Graphite Filled Polyaniline Composites and Evaluation of Their Electrical and Electrochemical Properties. *J Mater Sci: Mater Electron* **2011**, *22*, 1154–1161, doi:10.1007/s10854-010-0276-7.
25. Chulkin, P.; Łapkowski, M. An Insight into Ionic Conductivity of Polyaniline Thin Films. *Materials (Basel)* **2020**, *13*, 2877, doi:10.3390/ma13122877.
26. Anderson, M.R.; Mattes, B.R.; Reiss, H.; Kaner, R.B. Conjugated Polymer Films for Gas Separations. *Science* **1991**, *252*, 1412–1415, doi:10.1126/science.252.5011.1412.
27. McVerry, B.; Anderson, M.; He, N.; Kweon, H.; Ji, C.; Xue, S.; Rao, E.; Lee, C.; Lin, C.-W.; Chen, D.; et al. Next-Generation Asymmetric Membranes Using Thin-Film Liftoff. *Nano Lett.* **2019**, *19*, 5036–5043, doi:10.1021/acs.nanolett.9b01289.
28. Kweon, H.; Lin, C.-W.; Faruque Hasan, M.M.; Kaner, R.; Sant, G.N. Highly Permeable Polyaniline–Graphene Oxide Nanocomposite Membranes for CO2 Separations. *ACS Appl. Polym. Mater.* **2019**, *1*, 3233–3241, doi:10.1021/acsapm.9b00426.
29. Park, C.; Johnston, A.S.; Kweon, H. Physical Filtration Efficiency Analysis of a Polyaniline Hybrid Composite Filter with Graphite Oxide for Particulate Matter 2.5. *Journal of Applied Polymer Science* **2020**, *137*, 49149, doi:10.1002/app.49149.
30. Ramasubramanian, B.; Reddy, M.V.; Zaghib, K.; Armand, M.; Ramakrishna, S. Growth Mechanism of Micro/Nano Metal Dendrites and Cumulative Strategies for Countering Its Impacts in Metal Ion Batteries: A Review. *Nanomaterials (Basel)* **2021**, *11*, 2476, doi:10.3390/nano11102476.
31. Fang, Y.; Zhang, S.L.; Wu, Z.-P.; Luan, D.; Lou, X.W. (David) A Highly Stable Lithium Metal Anode Enabled by Ag Nanoparticle–Embedded Nitrogen-Doped Carbon Macroporous Fibers. *Science Advances* **2021**, *7*, eabg3626, doi:10.1126/sciadv.abg3626.
32. Luo, J.; Lee, R.-C.; Jin, J.-T.; Weng, Y.-T.; Fang, C.-C.; Wu, N.-L. A Dual-Functional Polymer Coating on a Lithium Anode for Suppressing Dendrite Growth and Polysulfide Shuttling in Li–S Batteries. *Chem. Commun.* **2017**, *53*, 963–966, doi:10.1039/C6CC09248A.
33. Ji, X.; Nazar, L.F. Advances in Li–S Batteries. *J. Mater. Chem.* **2010**, *20*, 9821–9826, doi:10.1039/B925751A.
34. Zhang, B.; Qin, X.; Li, G.R.; Gao, X.P. Enhancement of Long Stability of Sulfur Cathode by Encapsulating Sulfur into Micropores of Carbon Spheres. *Energy Environ. Sci.* **2010**, *3*, 1531–1537, doi:10.1039/C002639E.
35. Deng, Z.; Zhang, Z.; Lai, Y.; Liu, J.; Li, J.; Liu, Y. Electrochemical Impedance Spectroscopy Study of a Lithium/Sulfur Battery: Modeling and Analysis of Capacity Fading. *J. Electrochem. Soc.* **2013**, *160*, A553, doi:10.1149/2.026304jes.